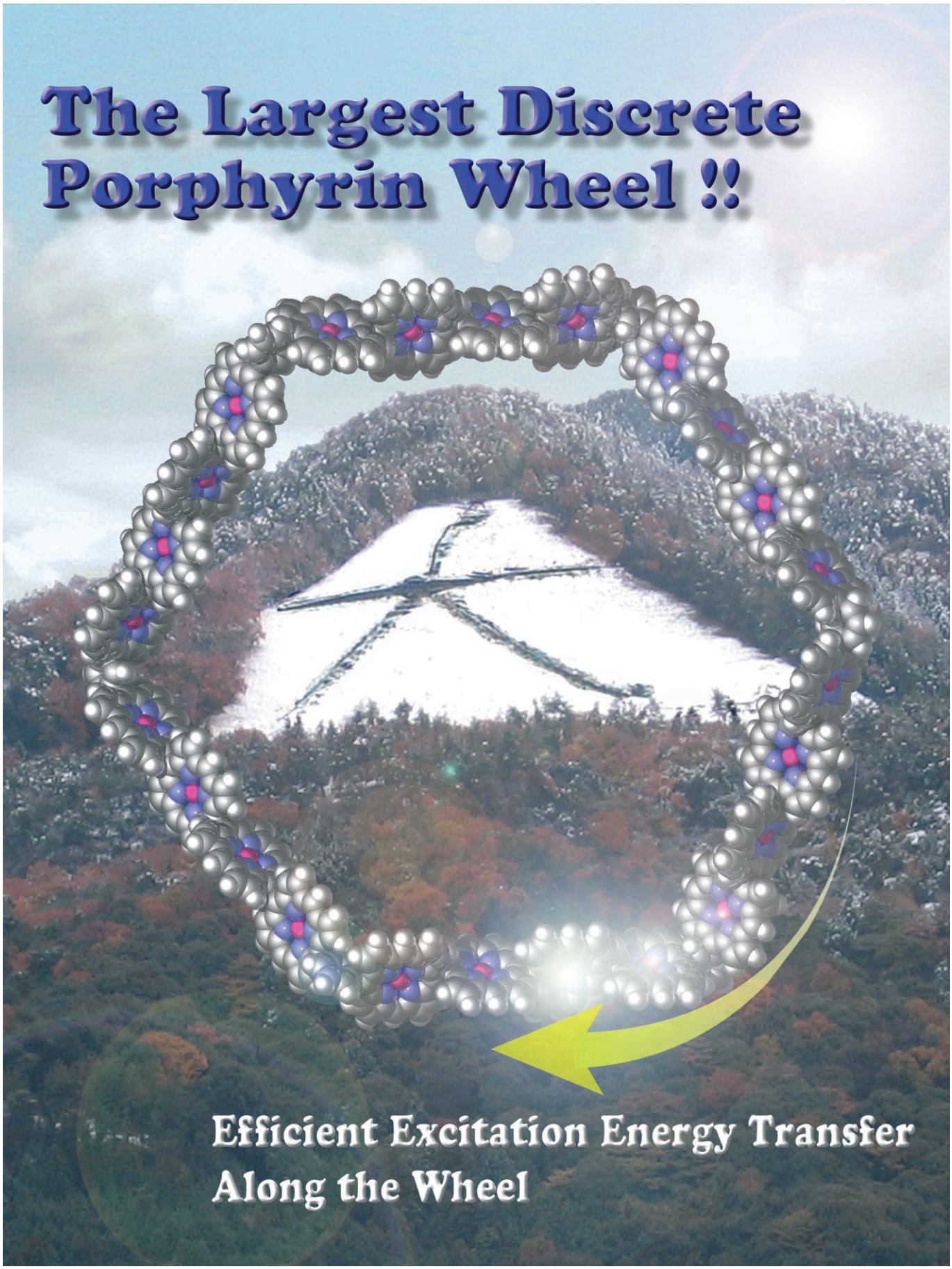

CHEMISTRY
A EUROPEAN JOURNAL

DOI: 10.1002/chem.200501373

Giant Porphyrin Wheels with Large Electronic Coupling as Models of Light-Harvesting Photosynthetic Antenna

Takaaki Hori,[a] Naoki Aratani,[a] Akihiko Takagi,[b] Takuya Matsumoto,*[b] Tomoji Kawai,*[b] Min-Chul Yoon,[c] Zin Seok Yoon,[c] Sung Cho,[c] Dongho Kim,*[c] and Atsuhiro Osuka*[a]

Abstract: Starting from a 1,3-phenylene-linked diporphyrin zinc(II) complex **2ZA**, repeated stepwise Ag^{I}-promoted coupling reactions provided linear oligomers **4ZA**, **6ZA**, **8ZA**, and **12ZA**. The intramolecular cyclization reaction of **12ZA** under dilute conditions (1×10^{-6} M) gave porphyrin ring **C12ZA** with a diameter of approximately 35 Å in 60% yield. This synthetic strategy has been applied to a 1,3-phenylene-linked tetraporphyrin **4ZB** to provide **8ZB**, **12ZB**, **16ZB**, **24ZB**, and **32ZB**. The intramolecular coupling reaction of **24ZB** gave a larger 24-mer porphyrin ring **C24ZB** with a diameter of approximately 70 Å in 34% yield. These two large porphyrin rings were characterized by means of ^{1}H NMR spectroscopy, matrix-assisted laser desorption ionization time-of-flight (MALDI-TOF) mass spectroscopy, UV-visible spectroscopy, gel permeation chromatography (GPC) analysis, and scanning tunneling microscopy (STM) techniques. The STM images of **C12ZA** reveal largely circular structures, whereas those of **C24ZB** exhibit mostly ellipsoidal shapes, indicating more conformational flexibility of **C24ZB**. Similar to the case of **C12ZA**, the efficient excitation energy transfer along the ring has been confirmed for **C24ZB** by using the time-correlated single-photon counting (TCSPC) and picosecond transient absorption anisotropy (TAA) measurements, and occurs with a rate of $(35\text{ ps})^{-1}$ for energy hops between neighboring tetraporphyrin subunits. Collectively, the present work provides an important step for the construction of large cyclic-arranged porphyrin arrays with ample electronic interactions as a model of light-harvesting antenna.

Keywords: energy transfer · nanostructures · oligomerization · photosynthetic antenna · porphyrinoids

[a] T. Hori, Dr. N. Aratani, Prof. Dr. A. Osuka
Department of Chemistry, Graduate School of Science
Kyoto University, and Core Research for Evolutional Science and Technology (CREST), Japan Science and Technology Agency
Sakyo-ku, Kyoto 606-8502 (Japan)
Fax: (+81) 75-753-3970
E-mail: osuka@kuchem.kyoto-u.ac.jp

[b] Dr. A. Takagi, Prof. T. Matsumoto, Prof. T. Kawai
The Institute of Scientific and Industrial Research (ISIR)
Osaka University, and Core Research for Evolutional Science and Technology (CREST), Japan Science and Technology Agency
8-1, Mihogaoka, Ibaragi, 567-0047 Osaka (Japan)
Fax: (+81) 66-875-2440
E-mail: matsumoto@sanken.osaka-u.ac.jp
kawai@sanken.osaka-u.ac.jp

[c] M.-C. Yoon, Z. S. Yoon, S. Cho, Prof. Dr. D. Kim
Center for Ultrafast Optical Characteristics Control and Department of Chemistry
Yonsei University, Seoul 120-749 (Korea)
Fax: (+82) 2-2123-2434
E-mail: dongho@yonsei.ac.kr

Supporting information for this article is available on the WWW under http://www.chemeurj.org/ or from the author.

Introduction

A variety of covalently linked porphyrin arrays have been explored as biomimetic models of photosynthetic systems, photonic materials, and functional molecular devices.[1,2] Among these, the design and synthesis of light-harvesting antenna systems that rival those in photosynthesis has been a long-standing issue, which requires the organization of many pigments in a designed regular arrangement. Inspired by the wheel-like giant architecture of photosynthetic pigments (LH2 and LH1),[3] particular attention has been focused on the construction of cyclic porphyrin arrays, which may aid the understanding of the fundamental mechanisms of excitation energy transfer in the natural photosynthetic antenna and/or find use as optoelectronic material.[4–10] The synthetic porphyrin wheels prepared so far contain at most twelve porphyrin units,[8,10] whereas LH2 consists of two wheel-like pigment arrays; B800 with nine bacteriochlorophyll *a* (Bchl *a*) and B850 with nine dimeric subunits (total 18 pigments) of Bchl *a*, hence posing a further synthetic

challenge. Furthermore, the absorption of a photon by the B850 ring is often described in terms of an excitation that is delocalized over the ring with a coherence length of four,[11] which requires ample electronic coupling in the molecular design to achieve high-performing artificial antenna.

In the last decade, we have explored the Ag^{I}-promoted *meso–meso* coupling reaction of Zn^{II}–5,15-diarylporphyrins,[12a] which is quite a powerful reaction and enables the syntheses of a variety of porphyrin arrays including three-dimensional windmill porphyrin arrays[12b,c] and a series of extremely long yet discrete *meso–meso*-linked porphyrin arrays.[12d] On the basis of this coupling reaction, a dodecameric porphyrin wheel **C12ZA** has been explored, in which six *meso–meso*-linked zinc(II)–diporphyrin subunits are bridged by 1,3-phenylene spacers.[13] Efficient excitation energy transfer along **C12ZA**, which has been confirmed by the measurements of femtosecond transient absorption anisotropy decay and the exciton–exciton annihilation lifetime, is aided by large electronic coupling between the neighboring *meso–meso*-linked diporphyrin subunits. As an extension, we report here the improved synthesis of **C12ZA**, the synthesis of 24-mer 1,3-phenylene-linked porphyrin ring **C24ZB**, and the excited-state dynamics of **C24ZB** relative to those of its linear counterpart **24ZB**. It is interesting to note that the radiative coherence length in *meso–meso*-linked porphyrin arrays has been experimentally estimated to be about four,[14] being similar to that in LH2.[11]

Results and Discussion

The synthetic scheme of **C12ZA** is shown in Scheme 1. Diporphyrin **2ZA** was prepared by Suzuki–Miyaura coupling of boronate **1** with 1,3-diiodobenzene.[15,16] To a solution of **2ZA** (0.2 mM) in freshly distilled $CHCl_3$, $AgPF_6$ (1.0 equiv) was added and the resulting mixture was stirred for five minutes at room temperature. Progress of the reaction was monitored by matrix-assisted laser desorption ionization time-of-flight (MALDI-TOF) mass spectroscopy. After the usual workup,[12a,d] the products were separated by using size-exclusion chromatography to give porphyrin tetramer **4ZA** (28%), hexamer **6ZA** (11%), and octamer **8ZA** (3–5%). Similarly, coupling of **4ZA** gave **8ZA** (29%), **12ZA** (14%), and **16ZA** (4–6%), and that of **8ZA** gave **16ZA** (25%), **24ZA** (8%), and **32ZA** (3%). It is noteworthy that the coupling regio-selectivity is always very high, only occurring at *meso–meso* positions. As is the case for the *meso–meso*-linked porphyrin arrays,[12,17] these porphyrin products have sufficient solubility in $CHCl_3$ and THF and the separation of long arrays was aided by a large difference in molecular size by using preparative gel permeation chromatography/high-pressure liquid chromatography (GPC–HPLC). The molecular length of **32ZA**, a 32-mer porphyrin, is estimated to be approximately 26 nm in its linear form. All these products have been fully characterized by means of ^{1}H NMR, mass, UV-visible, and fluorescence spectroscopy measurements. The linear porphyrin array **12ZA** was coupled to give **C12ZA** under highly dilute conditions, initially in 12% yield along with the recovery of **12ZA** (51%)[13] and now in an improved yield of 60% along with the recovery of **12ZA** (25%).

The synthetic route to **24ZB** is shown in Scheme 2. The *meso–meso*-linked diporphyrin boronate **3** was prepared from *meso–meso*-linked diporphyrin **2** via a partially brominated diporphyrin, in 46% yield. 1,3-Phenylene-bridged tetraporphyrin **4ZB** was prepared in 46% yield by Suzuki–

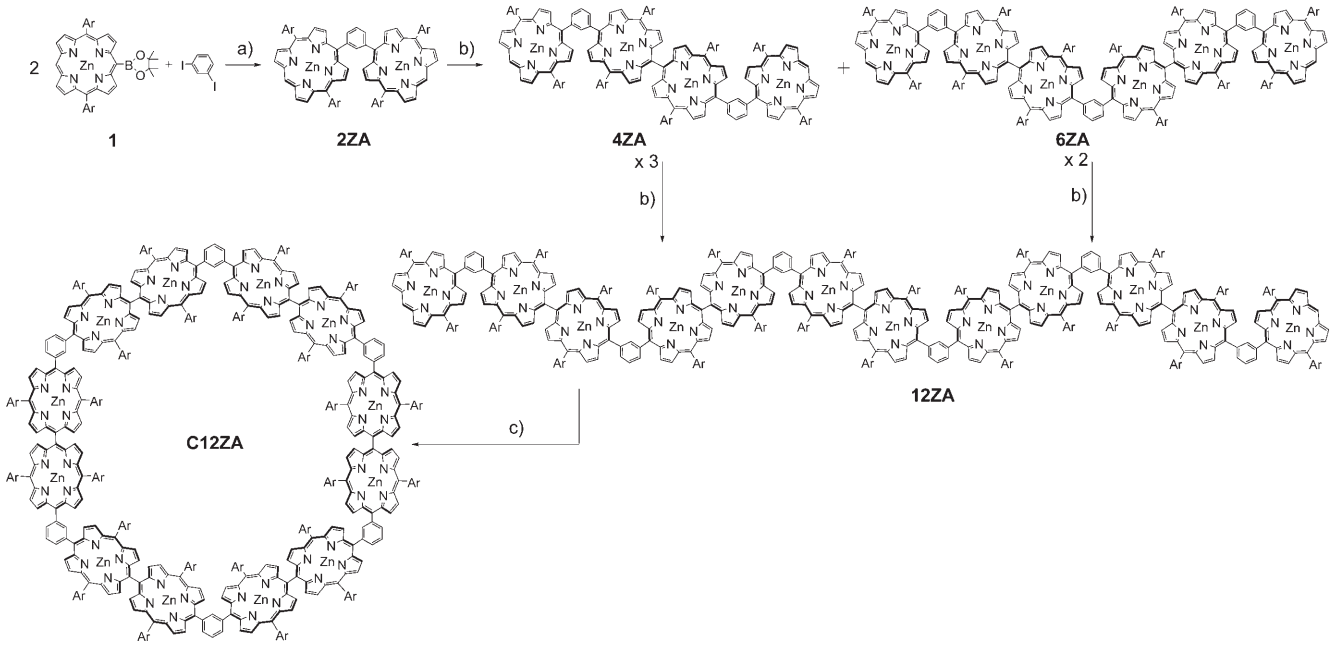

Scheme 1. Synthesis of **C12ZA** from **12ZA**. a) $[PdCl_2(PPh_3)_2]$, $AsPh_3$, Cs_2CO_3, DMF. b) $AgPF_6$ (0.7 equiv), $CHCl_3$. c) $AgPF_6$ (3.0 equiv), $CHCl_3$. Ar = *p*-dodecyloxyphenyl.

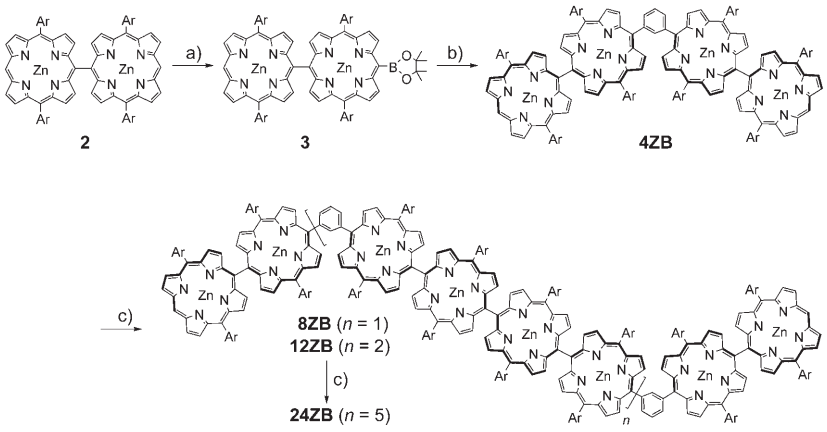

Scheme 2. A modular approach to the construction of 1,3-phenylene-bridged *meso–meso*-linked tetraporphyrin oligomers. a) 1) NBS, 2) pinacolborane, $[PdCl_2(PPh_3)_2]$, NEt_3, dichloroethane. b) 1,3-diiodobenzene, $[PdCl_2(PPh_3)_2]$, $AsPh_3$, Cs_2CO_3, DMF. c) $AgPF_6$, $CHCl_3$. Ar = *p*-dodecyloxyphenyl.

Miyaura coupling of **3** with 1,3-diiodobenzene.[15] To a solution of **4ZB** in $CHCl_3$ (1.0 mM), $AgPF_6$ (0.7 equiv) was added and the resulting mixture was stirred for two minutes at room temperature. After the usual workup,[12a,d] the products were separated by using size-exclusion chromatography to give porphyrin octamer **8ZB** (29%), dodecamer **12ZB** (10%), along with recovered **4ZB** (56%). In the next step, a solution of **8ZB** (1.0 mM) was treated with $AgPF_6$ (0.7 equiv) for two minutes at room temperature. The separation by using preparative GPC–HPLC gave hexadecamer **16ZB** (27%), and tetracosamer **24ZB** (10%). Similar coupling of **12ZB** gave **24ZB** in 11% yield. All these products have also been characterized by means of ^1H NMR, MALDI-TOF mass, UV-visible, and fluorescence spectroscopy as well as by GPC analysis. In particular, the MALDI-TOF MS technique is a powerful analytical tool for confirmation of molecular structures of this size.

Following this we examined the intramolecular cyclization of **24ZB** to **C24ZB** (Scheme 3). Under highly dilute conditions (1×10^{-6} M), **24ZB** was treated with three equivalents of $AgPF_6$ for 60 h at room temperature. Progress of the reaction was monitored by analytical GPC–HPLC, which revealed the formation of a discrete product that eluted as a new peak at 17.8 min, slower than **24ZB** at 17.1 min, hence indicating its smaller hydrodynamic volume (Figure 1). This product was isolated by repeated preparative GPC–HPLC analyses in 34% yield and has been assigned to a wheel-like tetracosameric porphyrin array (**C24ZB**) on the basis of the following facts: 1) The product exhibits the parent ion peak at 21880 (m/z calcd for $C_{1380}H_{1608}N_{96}O_{48}Zn_{24}$: 21878) along with a small dicationic peak in the MALDI-TOF mass spectrum (Figure 2), thus indicating its porphyrin 24-mer constitution. 2) Despite a small difference in the molecular weight (only 2 over 21878), a distinct difference in the retention time on the GPC–HPLC chromatography from **24ZB** indicates a substantial difference in the hydrodynamic volume, which will be related to an overall drastic change in molecular shape. 3) Although

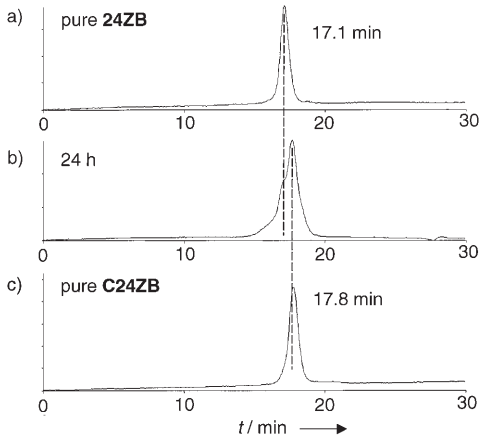

Figure 1. GPC–HPLC chromatographic charts: a) **24ZB**, b) reaction mixture of **24ZB** with $AgPF_6$ for 24 h, and c) purified **C24ZB**.

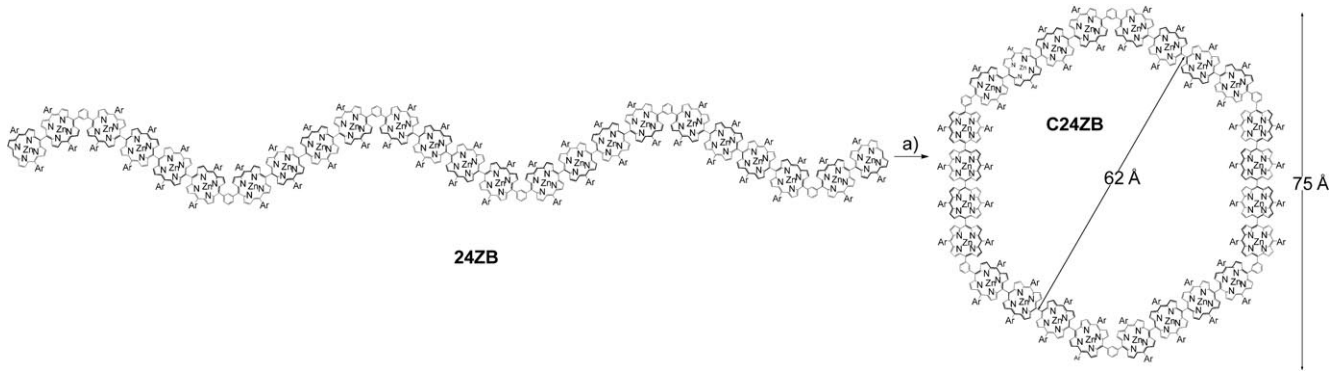

Scheme 3. Synthesis of **C24ZB** from **24ZB**. a) 3.0 equiv of $AgPF_6$, $CHCl_3$. Ar = *p*-dodecyloxyphenyl.

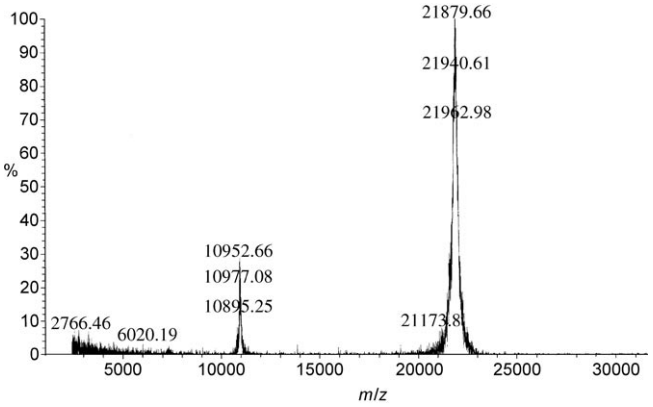

Figure 2. MALDI-TOF mass spectra of **C24ZB**.

the ^{1}H NMR spectrum is rather broadened, no *meso*-proton signal is observed (Figure 3). 4) The absorption spectrum of **C24ZB** is unique in the sense that the Soret band at around $\lambda = 460$ nm disappears as a consequence of its symmetric wheel structure without edge diporphyrins (Figure 4a). The ^{1}H NMR spectra of **12ZB**, **24ZB**, and **C24ZB** are shown in Figure 3. The proton signals of **12ZB** and **24ZB** that have been assigned by extensive two-dimensional COSY and NOESY techniques indicate the presence of the edge *meso* protons at $\delta = 10.34$ and 10.36 ppm and thus their linear structures. In contrast, the ^{1}H NMR spectrum of **C24ZB** does not show signals due to the edge *meso* protons, in line with its cyclic structure, but is considerably broad, presumably reflecting a slower rotational movement and/or the existence of several pseudostable conformations in solution. The ^{1}H NMR spectrum is independent of temperature in the range of -50 to 100 °C.

The UV-visible absorption spectra of **4ZB**, **24ZB**, and **C24ZB** are shown in Figure 4a. The absorption spectra of **24ZB** and **C24ZB** reveal increased absorbance with the increase of the number of porphyrin units relative to that of **4ZB**. In addition, the splitting energy of the Soret bands due to exciton coupling in **4ZB** ($\tilde{\nu} \approx 2393$ cm^{-1}) becomes larger ($\tilde{\nu} \approx 3713$ cm^{-1}) for **24ZB** and **C24ZB** (Table 1). Although the absorption spectra of **24ZB** and **C24ZB** have different shapes in the low-energy Soret bands, their absorbance in the Q-band region is almost the same.

The fluorescence spectra for **C24ZB** and **24ZB** are quite similar (Figure 4b), as are the fluorescence quantum yields ($\Phi_F = 0.03$). The fluorescence lifetimes measured by means of the time-correlated single-photon counting (TCSPS) technique are $\tau_F = 1.58 \pm 0.02$ ns for **8ZC** and $\tau_F = 1.63 \pm 0.02$ ns for **4ZC** (Table 1, Scheme 4). It is noteworthy that **C24ZB** showed an additional short decay component ($\tau_F = 0.11 \pm 0.03$ ns, 76 %) as well as a normal decay component ($\tau_F = 1.53 \pm 0.03$ ns, 24 %), which is not observed in **8ZC** or **4ZC** and may be assigned to the fluorescence quenching due to conformational heterogeneity that is imposed upon forming a large cyclic porphyrin array (Figure 5a).[20]

Figure 6 shows the scanning tunneling microscopy (STM) images of **C24ZB** taken with a sample bias (V_s) of 1.5 V and a tunneling current (I_t) of 12.8 pA that reveal discrete elliptic rings with hollows. These deformed images ascertain conformational flexibility compared with rather uniform

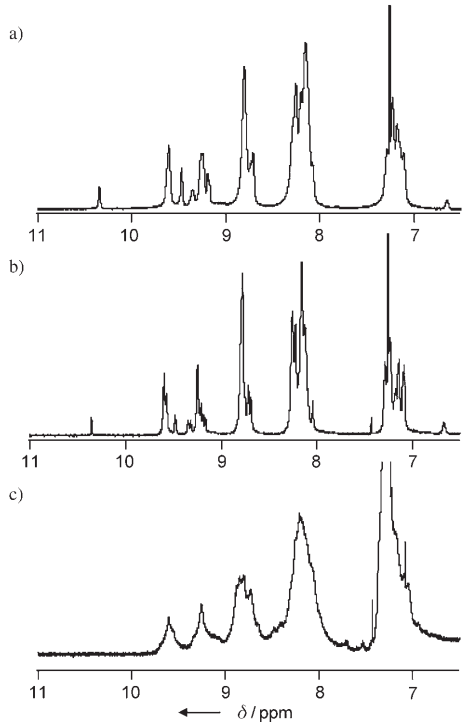

Figure 3. ^{1}H NMR spectra of a) **12ZB**, b) **24ZB**, and c) **C24ZB** in $CDCl_3$.

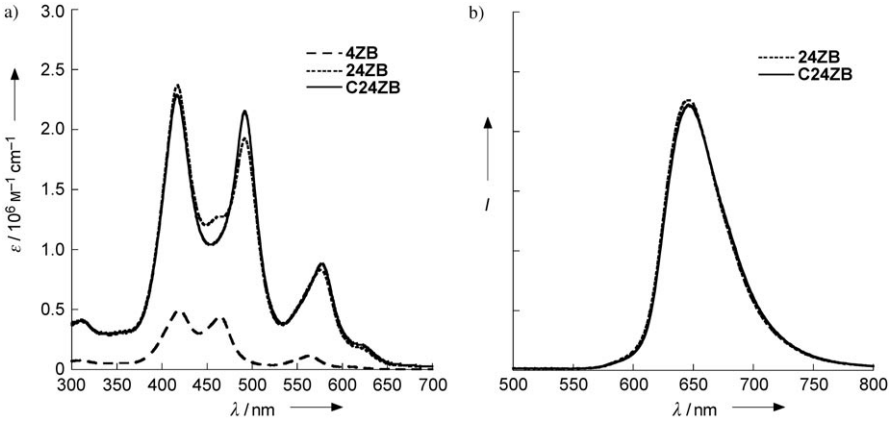

Figure 4. a) UV/Vis absorption spectra of **4ZB**, **24ZB**, and **C24ZB**, and b) fluorescence spectra of **24ZB** and **C24ZB** in $CHCl_3$.

Table 1. Photophysical properties of **4ZC**, **8ZC**, and **C24ZB**.

	λ_{abs} [nm][a]			λ_{em} [nm][b]		τ_F [ns][c]	τ_r [ps][d]	r_0[e]	r_{inf}[f]
4ZC	416	488	570	612	639	–	1.63±0.02	–	0.27	0.26
8ZC	416	491	571	613	640	–	1.58±0.02	16.3±0.1	0.22	0.1
C24ZB	417	493	572	615	643	0.11±0.03	1.53±0.03	11.7±0.1	0.21	0.07

[a] Absorption wavelength. [b] Fluorescence wavelength. [c] Fluorescence lifetime. [d] Anisotropy delay time constant. [e] Anisotropy value at $t=0$. [f] Anisotropy value at $t=130$ ps.

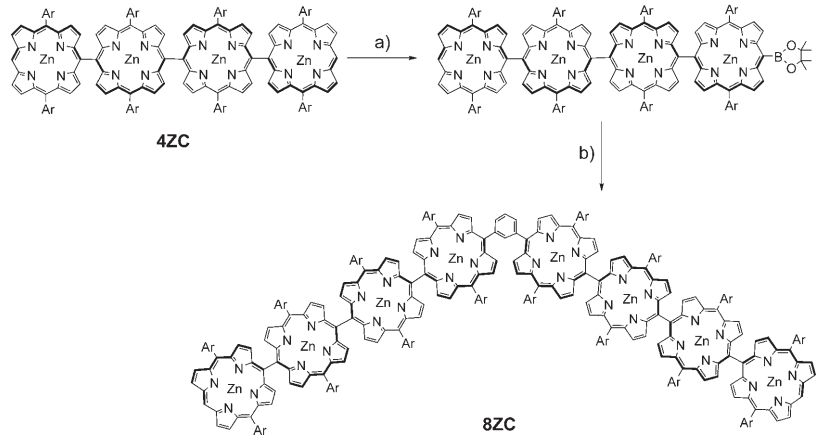

Scheme 4. Synthesis of **8ZC**. a) 1) NBS, 2) pinacolborane, $[PdCl_2(PPh_3)_2]$, NEt_3, dichloroethane. b) 1,3-diidobenzene, $[PdCl_2(PPh_3)_2]$, $AsPh_3$, Cs_2CO_3, DMF. Ar = *p*-dodecyloxyphenyl.

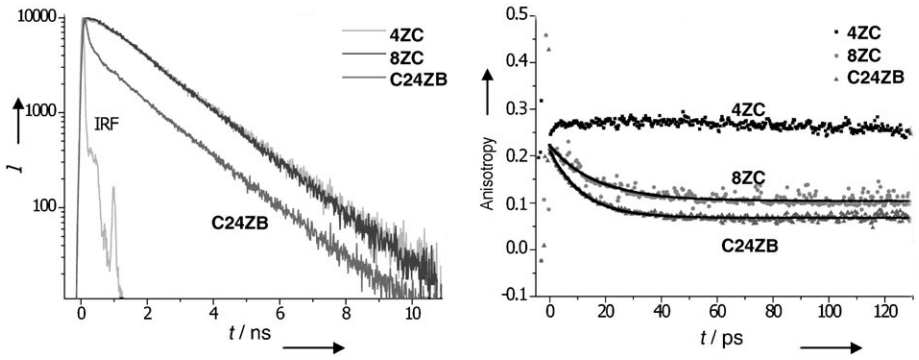

Figure 5. Fluorescence decay (left) and transient absorption anisotropy decay (right) of **4ZC**, **8ZC**, and **C24ZB**.

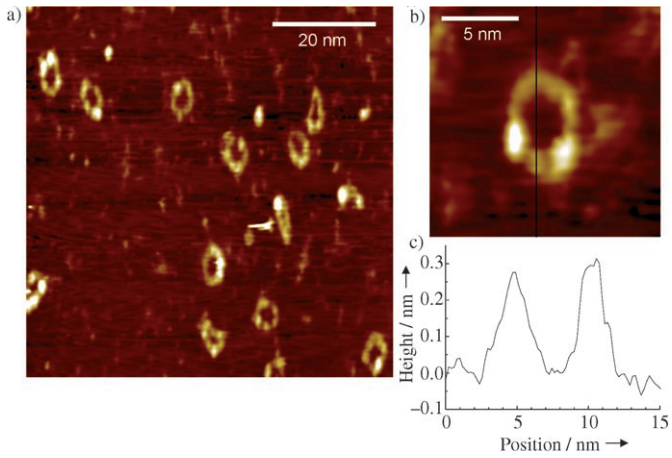

Figure 6. a) STM images of **C24ZB** on Cu(100) surface. b) Enlarged image of **C24ZB**. c) A cross section along the line shown in b).

C12ZA (ca. 35 Å diameter). The averaged diameter of the STM images of **C24ZB** is 45–70 Å, which matches roughly with its calculated diameter (ca. 70 Å, Scheme 3).

The femtosecond time-resolved transient absorption anisotropy (TAA) measurements probed at 510 nm after the photoexcitation at 550 nm (Q band) revealed the decay components, 11.7±0.1 ps for **C24ZB** and 16.3±0.1 ps for **8ZC** (Table 1), which have been assigned to the excitation energy transfer (EET) processes between *meso–meso*-linked tetraporphyrin subunits bridged by a 1,3-phenylene spacer (Figure 5b). Because the EET in **8ZC** is reversible between tetraporphyrin units (**4Z**), the EET rate constants can be expressed as $\tau=1/(k_1+k_{-1})$, in which τ is the measured anisotropy decay time of **8ZC** and k_1 and k_{-1} are the forward and reverse reaction rate constants, respectively. According to this relation, the EET rate constant via the 1,3-phenylene spacer of **8ZC** was determined to be $(32.6\ \text{ps})^{-1}$. On the other hand, tetraporphyrin subunits (**4Z**) in **C24ZB** are arranged in a cyclic form with six tetraporphyrin units (**4Z**). When the Förster-type incoherent energy-hopping model is employed for this EET mechanism, the depolarization times are related to the EET time by $\tau_{depolarization}=\tau_{EET}/3$.[21,22] Overall, the EET time constant in **C24ZB** has been calculated to be $3\times11.7=35.1$ ps (Scheme 5). Interestingly, the slower EET rate in **C24ZB** relative to that in **C12ZA** $(3.6\ \text{ps})^{-1}$ is consistent with their molecular architectures in that the center-to-center distance between the adjacent tetraporphyrin subunits (**4Z**) in **C24ZB** is roughly 1.5 times longer than that in **C12ZA**. As the EET rate can be related to the center-to-center distance (R) by $k_{EET}\propto R^{-6}$ in the Förster-type incoherent energy-hopping model, it is reasonable to observe a roughly ten times ($1.5^6=11.4$) slower EET rate for **C24ZB** than that for **C12ZA**.

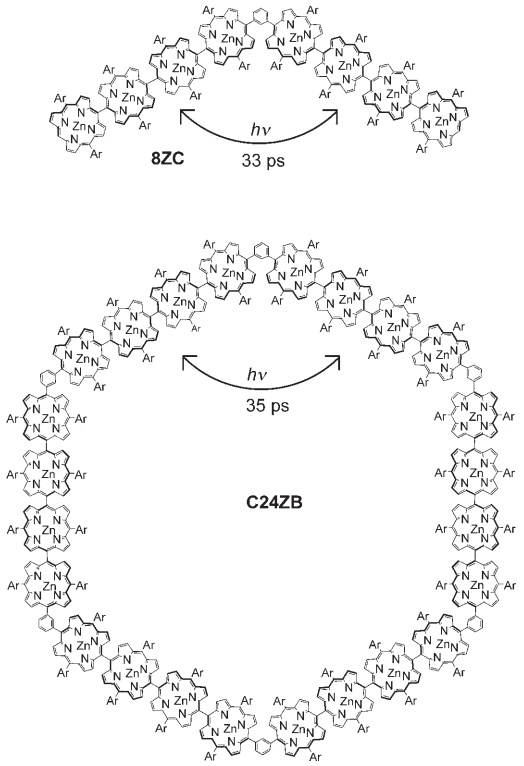

Scheme 5. Excitation energy transfer in **8ZC** and **C24ZB**.

Conclusion

The intramolecular Ag^{I}-promoted coupling of **24ZB** under high dilution conditions afforded the giant wheel-like porphyrin array **C24ZB** comprising of six *meso–meso*-linked tetraporphyrins. **C24ZB** exhibits an efficient excitation energy hopping rate of $(35.1\,\mathrm{ps})^{-1}$ along the array, as revealed by the time-resolved fluorescence decay and transient absorption anisotropy decay measurements. The **C24ZB** wheel has a diameter of approximately 7 nm and is, to the best of our knowledge, the largest covalently linked porphyrin ring. Exploration of even larger porphyrin wheels such as 36 (6×6) porphyrin units as an LH1 model, and fabrication of these arrays with an appropriate electron acceptor are subjects of further investigation.

Experimental Section

General procedures: All reagents and solvents were of commercial reagent grade and were used without further purification except when noted otherwise. Dry toluene and CH_2Cl_2 were obtained by distillation over CaH_2. ^{1}H NMR spectra were recorded on a JEOL ECA-delta-600 spectrometer, and chemical shifts were reported as the delta scale in ppm relative to $CHCl_3$ (N.B. Ar = *p*-dodecyloxyphenyl). The spectroscopic grade $CHCl_3$ was used as solvent for all spectroscopic studies. UV/Vis absorption spectra were recorded on a Shimadzu UV-3100 spectrometer. Steady-state fluorescence emission spectra were recorded on a Shimadzu RF-5300PC spectrometer. Mass spectra were recorded on a Shimadzu/KRATOS KOMPACT MALDI 4 spectrometer, using a positive-MALDI ionization method with/without a dithranol matrix. Preparative separations were performed by means of silica gel flash column chromatography (Merck Kieselgel 60H Art. 7736) and silica gel gravity column chromatography (Wako gel C-300). Recycling preparative GPC–HPLC was carried out on a JAI LC-908 apparatus using preparative JAIGEL-2.5H, 3H, and 4H columns (chloroform as eluant; flow rate 3.8 mL min^{-1}).

Synthesis: Although synthetic procedures of compounds **1**, **2ZA**–**12ZA**, and **C12ZA** were reported previously,[13] now much improved yields have been achieved by slightly modifying the procedures. In the cyclization reaction from **12ZA** to **C12ZA**, the reaction solvent (1.0 L $CHCl_3$) was distilled from CaH_2, passed through an active alumina column, and degassed by argon bubbling before use. The oxidative coupling reaction of **12ZA** (24 mg, 2.1 μmol) in an inert atmosphere with an amplified addition of $AgPF_6$ (6.4 μmol, 3.0 equiv) caused an increase in the isolated yield (14 mg, 60 %).

Boronate porphyrin ***3***: Compound **2** (1.05 g, 0.56 mmol) was dissolved in a mixture of $CHCl_3$ (500 mL) and pyridine (0.5 mL). NBS (140 mg, 0.79 mmol) was added to this solution and the resulting solution was stirred for 15 min at 0 °C. The mixture was poured into water and extracted with $CHCl_3$. The combined organic extract was dried over Na_2SO_4. The solvent was removed by using a rotary evaporator and the residue was recrystallized from $CHCl_3/CH_3CN$. A flask was charged with a mixture of bromoporphyrins, pinacolborane (0.65 mL, 4.47 mmol), triethylamine (0.70 mL, 9.68 mmol), $[PdCl_2(PPh_3)_2]$ (13.4 mg, 0.019 mmol), and 1,2-dichloroethane (60 mL) under N_2. The mixture was stirred at 90 °C for 6 h. The reaction mixture was washed with water, and dried over Na_2SO_4. The solvent was evaporated, and the residue was taken up in CH_2Cl_2. Compound **3** was purified by silica gel flash column chromatography using CH_2Cl_2/hexane as the eluant. The first band isolated corresponded to **2**, while the second band was the porphyrin boronate **3** (493 mg, 46 %). ^{1}H NMR ($CDCl_3$, 600 MHz): δ = 10.34 (s, 1H; *meso*-H), 9.97 (d, J = 4.6 Hz, 2H; β-H), 9.46 (d, J = 4.6 Hz, 2H; β-H), 9.17 (m, 4H; β-H), 8.71 (d, J = 4.6 Hz, 2H; β-H), 8.67 (d, J = 4.6 Hz, 2H; β-H), 8.08–8.12 (m, 12H; 8×Ar, 4×β-H), 7.18 (t, J = 8.7 Hz; Ar), 4.15 (t, J = 6.4 Hz, 8H; dodecyloxy), 1.89 (m, 20H; dodecyloxy + Me), 1.53–1.25 (m, 72H; dodecyloxy), 0.90 ppm (t, J = 6.8 Hz, 12H; dodecyloxy); MALDI-TOF MS: *m*/*z* calcd for $C_{118}H_{145}B_1N_8O_6Zn_2$: 1913; found: 1912.

Compound ***4ZB***: Boronate porphyrin **3** (535 mg, 0.279 mmol) was mixed with 1,3-diiodobenzene (46 mg, 0.140 mmol), Cs_2CO_3 (236 mg), $[PdCl_2(PPh_3)_2]$ (33 mg), and $AsPh_3$ (32 mg) in DMF. The mixture was degassed three times by freeze–pump–thaw cycles and stirred at 80 °C for 6 h. Then the mixture was washed with water, extracted with $CHCl_3$, dried over Na_2SO_4, and the solvent was evaporated to leave the residue that was passed through a short silica gel column. Separation over preparative GPC gave the coupling product **4ZB** (285 mg, 46 %). ^{1}H NMR ($CDCl_3$, 600 MHz): δ = 10.35 (s, 2H; *meso*-H), 9.54 (d, J = 4.6 Hz, 4H; β-H), 9.47 (t, 4H; β-H), 9.23 (s, 1H; 1,3-phenylene), 9.19–9.18 (m, 6H; β-H), 9.16 (d, 2H; β-H), 8.75–8.73 (m, 4H; β-H), 8.70–8.67 (m, 6H; 4×β-H, 2×1,3-phenylene), 8.23–8.05 (m, 25H; 16×Ar, 8×β-H, 1×1,3-phenylene), 7.28–7.16 (m, 16H; Ar), 4.18–4.12 (m, 16H; dodecyloxy), 1.94–1.85 (m, 16H; dodecyloxy), 1.53–1.24 (br m, 44H; dodecyloxy), 0.86–0.80 ppm (m, 24H; dodecyloxy); UV/Vis ($CHCl_3$): λ_{max} (ε) = 419 (490 000), 465 (437 000), 563 (111 000), 606 nm (22 000 mol^{-1} dm^3 cm^{-1}); MALDI-TOF MS: *m*/*z* calcd for $C_{230}H_{270}N_{16}O_8Zn_4$: 3648; found: 3646.

Compound ***8ZB***: ^{1}H NMR ($CDCl_3$, 600 MHz): δ = 10.38 (s, 2H; *meso*-H), 9.59–9.57 (m, 8H; β-H), 9.51–9.48 (m, 4H; β-H), 9.33 (s, 2H; 1,3-phenylene), 9.14–9.21 (m, 10H; 8×β-H, 2H×1,3-phenylene), 9.07 (d, 4H; β-H), 9.25–9.17 (m, 12H; β-H), 8.82–8.70 (m, 24H; 20×β-H, 4×1,3-phenylene), 8.32–8.07 (m, 54H; 32×Ar, 20×β-H, 2×1,3-phenylene), 7.28–7.08 (m, 32H; Ar), 4.22–4.06 (m, 32H; dodecyloxy), 1.98–1.78 (m, 32H; dodecyloxy), 1.58–1.14 (br m, 288H; dodecyloxy), 0.90–0.82 (m, 48H; dodecyloxy); UV/Vis ($CHCl_3$): λ_{max} (ε) = 418 (845 000), 460 (555 000), 490 (522 000), 571 nm (231 000 mol^{-1} dm^3 cm^{-1}); MALDI-TOF MS: *m*/*z* calcd for $C_{460}H_{538}N_{32}O_{16}Zn_8$: 7294; found: 7292.

Compound ***12ZB***: ^{1}H NMR ($CDCl_3$, 600 MHz): δ = 10.31 (s, 2H; *meso*-H), 9.57–9.54 (m, 12H; β-H), 9.56–9.54 (m, 4H; β-H), 9.32 (br s, 2H; 1,3-phenylene), 9.30 (br s, 1H; 1,3-phenylene), 9.21–9.12 (m, 16H; β-H), 8.73–8.62 (m, 42H; 36×β-H, 6×1,3-phenylene), 8.23–7.92 (m, 79H; 48×Ar, 28×β-H, 3×1,3-phenylene), 7.27–7.08 (m, 48H; Ar), 4.22–4.05 (m,

48H; dodecyloxy), 1.95–1.76 (m, 48H; dodecyloxy), 1.59–1.18 (br m, 432H; dodecyloxy), 0.87–0.76 ppm (m, 72H; dodecyloxy); UV/Vis ($CHCl_3$): λ_{max} (ε) = 418 (1270000), 461 (755000), 491 (853000), 575 nm (386000 $mol^{-1}dm^3cm^{-1}$); MALDI-TOF MS: *m/z* calcd for $C_{690}H_{806}N_{48}O_{24}Zn_{12}$: 10941; found: 10939.

Compound ***16ZB***: ^1H NMR ($CDCl_3$, 600 MHz): δ = 10.31 (s, 2H; *meso*-H), 9.60–9.57 (m, 16H; β-H), 9.48–9.46 (m, 4H; β-H), 9.35 (br s, 2H; 1,3-phenylene), 9.32 (br s, 2H; 1,3-phenylene), 9.25–9.15 (m, 20H; β-H), 8.75–8.67 (m, 64H; 56 × β-H, 8 × 1,3-phenylene), 8.27–8.07 (m, 100H; 64 × Ar, 32 × β-H, 4 × 1,3-phenylene), 7.30–7.10 (m, 64H; Ar), 4.26–4.04 (m, 64H; dodecyloxy), 1.92–1.78 (m, 64H; dodecyloxy), 1.60–1.12 (br m, 576H; dodecyloxy), 0.91–0.78 ppm (m, 96H; dodecyloxy); UV/Vis ($CHCl_3$): λ_{max} (ε) = 418 (1620000), 461 (915000), 492 (124000), 577 nm (535000 $mol^{-1}dm^3cm^{-1}$); MALDI-TOF MS: *m/z* calcd for $C_{920}H_{1074}N_{64}O_{32}Zn_{16}$: 14587; found: 14590.

Compound ***24ZB***: ^1H NMR ($CDCl_3$, 600 MHz): δ = 10.32 (s, 2H; *meso*-H), 9.59–9.57 (m, 24H; β-H), 9.48–9.44 (m, 4H; β-H), 9.34 (br s, 4H; 1,3-phenylene), 9.32 (br s, 2H; 1,3-phenylene), 9.15–9.24 (m, 28H; β-H), 8.78–8.68 (m, 98H; 86 × β-H, 12 × 1,3-phenylene), 8.27–8.05 (m, 152H; 96 × Ar, 50 × β-H, 6 × 1,3-phenylene), 7.36–7.10 (m, 96H; Ar), 4.25–4.08 (m, 96H; dodecyloxy), 1.98–1.80 (m, 96H; dodecyloxy), 1.75–1.12 (br m, 864H; dodecyloxy), 0.88–0.78 ppm (m, 144H; dodecyloxy); UV/Vis ($CHCl_3$): λ_{max} (ε) = 417 (2320000), 461 (1240000), 492 (1870000), 576 nm (809000 $mol^{-1}dm^3cm^{-1}$); MALDI-TOF MS: *m/z* calcd for $C_{1380}H_{1610}N_{96}O_{48}Zn_{24}$: 21880; found: 21877.

Compound ***C24ZB***: The reaction vessel containing a solution of **24ZB** (21 mg, 0.97 μmol) in freshly distilled $CHCl_3$ (500 mL) was covered with foil. A stock solution of $AgPF_6$ (2.9 μmol) in dry CH_3CN was added to the **24ZB** solution, which was stirred at room temperature under N_2, while the progress of the reaction was monitored by analytical GPC–HPLC. The reaction was stopped by adding water and the organic layer was separated and dried over anhydrous Na_2SO_4. A solution of $Zn(OAc)_2$ in methanol was added, and the resulting solution was stirred under reflux for 1–2 h. Then it was washed successively with water, saturated $NaHCO_3$ solution (aq), and saturated NaCl solution (aq), and dried over anhydrous Na_2SO_4. The solvent was removed by using a rotary evaporator to leave the residue, which was separated over a recycling preparative GPC–HPLC to give **24ZB** (4.0 mg, 23%) as the first fraction and **C24ZB** (7.0 mg, 34%) as the second fraction. ^1H NMR ($CDCl_3$, 600 MHz): δ = 9.75–9.40 (m, 12H; β-H), 9.40–8.90 (m, 22H; β-H + 1,3-phenylene), 8.90–8.60 (m, 58H; β-H + 1,3-phenylene), 8.60–7.80 (m, 220H; Ar + β-H + 1,3-phenylene), 7.40–6.90 (m, 96H; Ar), 4.30–4.00 (m, 96H; dodecyloxy), 2.10–0.80 ppm (m, 1104H; dodecyloxy); UV/Vis ($CHCl_3$): λ_{max} (ε) = 417 (2200000), 492 (2100000), 577 nm (868000 $mol^{-1}dm^3cm^{-1}$); MALDI-TOF MS: *m/z* calcd for $C_{1380}H_{1608}N_{96}O_{48}Zn_{24}$: 21878; found: 21880.

Compound **4ZC** was prepared by an Ag^I oxidative coupling reaction of the 5,15-bis(4-dodecyloxyphenyl)porphyrin–Zn^{II} complex.

Boronate tetraporphyrin ***4***: Compound **4ZC** (157 mg, 0.044 mmol) was dissolved in a mixture of $CHCl_3$ (100 mL) and pyridine (0.3 mL). NBS (11.7 mg, 0.066 mmol) was added to this solution and the resulting solution was stirred for 15 min at 0°C. The mixture was poured into water and extracted with $CHCl_3$. After the combined organic extract was dried over Na_2SO_4, the solvent was removed by using a rotary evaporator to leave the residue, which was recrystallized from a mixture of $CHCl_3$ and acetonitrile. A flask was charged with the mixture of bromoporphyrins, pinacolborane (0.7 mL, 4.8 mmol), triethylamine (0.8 mL, 11.1 mmol), $[PdCl_2(PPh_3)_2]$ (5 mg, 0.008 mmol), and 1,2-dichloroethane (30 mL) under N_2. The mixture was stirred at 90°C for 6 h. The reaction mixture was washed with water, and dried over Na_2SO_4. The solvent was evaporated, and the residue was taken up in CH_2Cl_2. The product **4** was purified by silica gel flash column chromatography using CH_2Cl_2/hexane as the eluant. The first band was **4ZC** and the second band was boronate **4** (21 mg, 13%). ^1H NMR ($CDCl_3$, 600 MHz): δ = 10.26 (s, 1H; *meso*-H), 9.93 (d, J = 4.6 Hz, 2H; β-H), 9.41 (d, J = 4.6 Hz, 2H; β-H), 9.11 (m, 4H; β-H), 8.72–8.60 (m, 12H; β-H), 8.20–7.98 (m, 28H; 12 × β-H, 16 × Ar), 7.30–7.18 (m, 16H; Ar), 4.12–3.98 (m, 16H; dodecyloxy), 1.93–1.82 (m, 28H; 16 × dodecyloxy, 12 × Me), 1.82–1.70 (m, 16H; dodecyloxy), 1.17–1.70 (br m, 128H; dodecyloxy), 0.92–0.78 ppm (m, 24H; dodecyloxy); MALDI-TOF MS: *m/z* calcd for $C_{230}H_{273}N_{16}O_{10}Zn_4$: 3687; found: 3685.

Compound ***8ZC***: The porphyrin tetramer **4** (20 mg, 0.0056 mmol) was mixed with 1,3-diiodobenzene (1 mg, 0.0027 mmol), Cs_2CO_3 (5 mg), $[PdCl_2(PPh_3)_2]$ (1 mg), and $AsPh_3$ (0.7 mg) in DMF. The mixture was degassed three times by freeze–pump–thaw cycles and stirred at 80°C for 6 h. Then the reaction mixture was washed with water, extracted with $CHCl_3$, dried over Na_2SO_4, and evaporated to leave the residue, which was separated by using preparative GPC. The first fraction was **8ZC** (3 mg, 12%). ^1H NMR ($CDCl_3$, 600 MHz): δ = 10.33 (s, 2H; *meso*-H), 9.58 (d, J = 4.6 Hz, 4H; β-H), 9.47 (d, J = 4.6 Hz, 4H; por-β-H), 9.33 (s, 1H; 1,3-phenylene), 9.22 (d, J = 4.6 Hz, 4H; β-H), 9.18 (d, J = 4.6 Hz, 4H; β-H), 8.77–8.65 (m, 26H; 24 × β-H, 2 × 1,3-phenylene), 8.25–8.08 (m, 57H; 24 × β-H, 1 × 1,3-phenylene, 32 × Ar), 7.30–7.08 (m, 32H; Ar), 4.20–4.12 (m, 32H; dodecyloxy), 2.02–1.88 (m, 32H; dodecyloxy), 1.88–1.75 (m, 32H; dodecyloxy), 1.77–1.18 (br m, 256H; dodecyloxy), 0.97–0.88 ppm (m, 48H; dodecyloxy); UV/Vis ($CHCl_3$): λ_{max} (ε) = 417 (671000), 490 (605000), 577 nm (240000 $mol^{-1}dm^3cm^{-1}$); MALDI-TOF MS: *m/z* calcd for $C_{454}H_{534}N_{32}O_{16}Zn_8$: 7219; found: 7218.

STM measurements: Clean, flat Cu(100) surfaces were obtained by Ar^+ sputtering and annealing (580°C) cycles for a substrate. The porphyrin-ring molecules dissolved into $CHCl_3$ were deposited by spraying approximately 0.5 μL of the solution onto the substrate under vacuum (10^{-6} mbar) using a pulse injection method, which is suited for deposition of large fragile molecules with escaping decomposition often encountered in sample deposition from the gas phase. In situ STM measurements were performed at room temperature under ultra-high vacuum ($< 10^{-10}$ mbar) with a home-built STM by using an electrochemical etched Pt/Ir tip. The STM image was obtained in a constant current mode.

Transient absorption spectroscopy: The dual-beam femtosecond time-resolved transient absorption spectrometer consisted of a self-mode-locked femtosecond Ti:sapphire oscillator (Coherent, MIRA), a Ti:sapphire regenerative amplifier (Clark MXR model TRA-1000) that was pumped by a Q-switched Nd:YAG laser (Clark MXR model ORC-1000), a pulse stretcher/compressor, an optical parametric amplifier (Clark MXR OPA), and an optical detection system. A femtosecond Ti:sapphire oscillator pumped by a cw Nd:YVO_4 laser (Coherent, Verdi) produced a train of ≈80 fs mode-locked pulses with an averaged power of 650 mW at 800 nm. The amplified output beam regenerated by chirped pulse amplification (CPA) had a pulse width of approximately 150 fs and a power of approximately 1 W at a repetition rate of 1 kHz, which was divided into two parts by a 1:1 beam splitter. One part was color-tuned for the pump beam by an optical parametric generation and amplification (OPG-OPA). The resulting laser pulse had a temporal width of ≈150 fs in the Vis/IR range. The pump beam was focused to a spot diameter of ≈1 mm, and the laser fluence was adjusted, using a variable neutral-density filter. The other part was focused onto a flowing water cell to generate a white-light continuum, which was again split into two parts. One part of the white-light continuum was overlapped with the pump beam at the sample to probe the transient, while the other part of the white-light continuum was passed through the sample without overlapping the pump beam. The time delay between pump and probe beams was controlled by making the pump beam travel along a variable optical delay line. The white-light continuum beams after the sample were sent through an appropriate interference filter and were then detected by two photodiodes. The outputs from the two photodiodes at the selected wavelength were processed by a combination of a boxcar averager and a lock-in amplifier, to calculate the absorption difference at the desired time delay between pump and probe pulses.

Acknowledgements

The work at Kyoto University was partly supported by the Grant-in-Aid from the Ministry of Education, Culture, Sports, Science and Technology, Japan (No. 16750117). The work at Yonsei University was supported by the Creative Research Initiatives Program of the Ministry of Science and Technology of Korea.

[1] a) M. R. Wasielewski, *Chem. Rev.* **1992**, *92*, 435; b) D. Gust, T. A. Moore, A. L. Moore, *Acc. Chem. Res.* **1993**, *26*, 198; c) S. Anderson, H. L. Anderson, J. K. M. Sanders, *Acc. Chem. Res.* **1993**, *26*, 469; d) D. F. Holten, D. Bocian, J. S. Lindsey, *Acc. Chem. Res.* **2002**, *35*, 57; e) A. K. Burrell, D. L. Officer, P. G. Plieger, D. C. W. Reid, *Chem. Rev.* **2001**, *101*, 2751; f) E. K. L. Yeow, K. P. Ghiggino, J. N. H. Reek, M. J. Crossley, A. W. Bosman, A. P. H. J. Schenning, E. W. Meijer, *J. Phys. Chem. B* **2000**, *104*, 2596; g) M.-S. Choi, T. Aida, Y. Yamazaki, I. Yamazaki, *Chem. Eur. J.* **2002**, *8*, 2668.

[2] a) N. Aratani, A. Osuka, *Bull. Chem. Soc. Jpn.* **2001**, *74*, 1361; b) N. Aratani, A. Tsuda, A. Osuka, *Synlett* **2001**, 1663; c) N. Aratani, A. Osuka, H. S. Cho, D. Kim, *J. Photochem. Photobiol. C* **2002**, *3*, 25; d) D. Kim, A. Osuka, *J. Phys. Chem. A* **2003**, *107*, 8791; e) N. Aratani, A. Osuka, *Chem. Rec.* **2003**, *3*, 255; f) I.-W. Hwang, N. Aratani, A. Osuka, D. Kim, *Bull. Korean Chem. Soc.* **2005**, *26*, 1; g) D. Kim, A. Osuka, *Acc. Chem. Res.* **2004**, *37*, 735.

[3] a) G. M. McDermott, S. M. Prince, A. A. Freer, A. M. Hawthonthwaite-Lawless, M. Z. Papiz, R. J. Cogdell, M. W. Isaacs, *Nature* **1995**, *374*, 517; b) J. Koepke, X. Hu, C. Muenke, K. Schulten, H. Michel, *Structure* **1996**, *4*, 581.

[4] a) O. Mongin, A. Schuwey, M.-A. Vallot, A. Gossauer, *Tetrahedron Lett.* **1999**, *40*, 8347; b) O. Mongin, N. Hoyler, A. Gossauer, *Eur. J. Org. Chem.* **2000**, 1193; c) S. Rucareanu, O. Mongin, A. Schuwey, N. Hoyler, A. Gossauer, W. Amrein, H.-U. Hediger, *J. Org. Chem.* **2001**, *66*, 4973.

[5] a) R. W. Wagner, J. Seth, S. I. Yang, D. Kim, D. F. Bocian, D. Holten, J. S. Lindsey, *J. Org. Chem.* **1998**, *63*, 5042; b) J. Li, A. Ambroise, S. I. Yang, J. R. Diers, J. Seth, C. R. Wack, D. F. Bocian, D. Holten, J. S. Lindsey, *J. Am. Chem. Soc.* **1999**, *121*, 8927.

[6] a) H. A. M. Biemans, A. E. Rowan, A. Verhoeven, P. Vanoppen, L. Latterini, J. Foekema, A. P. H. J. Schenning, E. W. Meijer, F. C. De Schryver, R. J. M. Nolte, *J. Am. Chem. Soc.* **1998**, *120*, 11054; b) G. Schweitzer, G. De Belder, L. Latterini, Y. Kani, A. E. Rowan, R. J. M. Nolte, F. C. De Schryver, *Chem. Phys. Lett.* **1999**, *303*, 261.

[7] a) K. Sugiura, Y. Fujimoto, Y. Sakata, *Chem. Commun.* **2000**, 1105; b) A. Kato, K. Sugiura, H. Miyasaka, H. Tanaka, T. Kawai, M. Sugimoto, M. Yamashita, *Chem. Lett.* **2004**, *33*, 578.

[8] R. Takahashi, Y. Kobuke, *J. Am. Chem. Soc.* **2003**, *125*, 2372.

[9] a) M. Takase, R. Ismael, R. Murakami, M. Ikeda, D. Kim, H. Shinmori, H. Furuta, A. Osuka, *Tetrahedron Lett.* **2002**, *43*, 5157; b) H. S. Cho, H. Rhee, J. K. Song, C.-K. Min, M. Takase, N. Aratani, S. Cho, A. Osuka, T. Joo, D. Kim, *J. Am. Chem. Soc.* **2003**, *125*, 5849.

[10] Quite recently, Kobuke et al. reported gigantic porphyrin wheels that were linked through hingelike ferrocene linkages. Unfortunately, however, these electron-rich linkages precluded the observation of EET processes due to intramolecular electron transfer: a) O. Shoji, S. Okada, A. Satake, Y. Kobuke, *J. Am. Chem. Soc.* **2005**, *127*, 2201; b) O. Shoji, H. Tanaka, T. Kawai, Y. Kobuke, *J. Am. Chem. Soc.* **2005**, *127*, 8598.

[11] a) T. Pullerits, M. Chachisvilis, V. Sundström, *J. Phys. Chem.* **1996**, *100*, 10787; b) O. Kühn, V. Sundström, *J. Chem. Phys.* **1997**, *107*, 4154; c) T. Kakitani, A. Kimura, *J. Phys. Chem. A* **2002**, *106*, 2173.

[12] a) A. Osuka, H. Shimidzu, *Angew. Chem.* **1997**, *109*, 93; *Angew. Chem. Int. Ed. Engl.* **1997**, *36*, 135; b) A. Nakano, A. Osuka, I. Yamazaki, T. Yamazaki, Y. Nishimura, *Angew. Chem.* **1998**, *110*, 3172; *Angew. Chem. Int. Ed.* **1998**, *37*, 3023; c) A. Nakano, T. Yamazaki, Y. Nishimura, I. Yamazaki, A. Osuka, *Chem. Eur. J.* **2000**, *6*, 3254; d) N. Aratani, A. Osuka, Y. H. Kim, D. H. Jeong, D. Kim, *Angew. Chem.* **2000**, *112*, 1517; *Angew. Chem. Int. Ed.* **2000**, *39*, 1458; e) Y. H. Kim, D. H. Jeong, D. Kim, S. C. Jeoung, H. S. Cho, S. K. Kim, N. Aratani, A. Osuka, *J. Am. Chem. Soc.* **2001**, *123*, 76.

[13] X. Peng, N. Aratani, A. Takagi, T. Matsumoto, T. Kawai, I.-W. Hwang, T. K. Ahn, D. Kim, A. Osuka, *J. Am. Chem. Soc.* **2004**, *126*, 4468.

[14] N. Aratani, H. S. Cho, T. K. Ahn, S. Cho, D. Kim, H. Sumi, A. Osuka, *J. Am. Chem. Soc.* **2003**, *125*, 9668.

[15] a) A. G. Hyslop, M. A. Kellett, P. M. Iovine, M. J. Therien, *J. Am. Chem. Soc.* **1998**, *120*, 12676; b) P. M. Iovine, M. A. Kellett, N. P. Redmore, M. J. Therein, *J. Am. Chem. Soc.* **2000**, *122*, 8717.

[16] a) X. Zhou, K. S. Chan, *J. Org. Chem.* **1998**, *63*, 99; b) D. A. Shultz, H. Lee, R. K. Kumar, K. P. Gwaltney, *J. Org. Chem.* **1999**, *64*, 9124; c) T. Mizutani, K. Wada, S. Kitagawa, *J. Am. Chem. Soc.* **2001**, *123*, 6459.

[17] N. Aratani, A. Takagi, Y. Yanagawa, T. Matsumoto, T. Kawai, Z. S. Yoon, D. Kim, A. Osuka, *Chem. Eur. J.* **2005**, *11*, 3389.

[18] H. Tanaka, T. Nakagawa, T. Kawai, *Surf. Sci.* **1996**, *364*, L575.

[19] P. G. Seybold, M. Gouterman, *J. Mol. Spectrosc.* **1969**, *31*, 1.

[20] T. K. Ahn, Z. S. Yoon, I.-W. Hwang, J. K. Lim, H. Rhee, T. Joo, E. Sim, S. K. Kim, N. Aratani, A. Osuka, D. Kim, *J. Phys. Chem. B* **2005**, *109*, 11223.

[21] I.-W. Hwang, D. M. Ko, T. K. Ahn, Z. S. Yoon, D. Kim, X. Peng, N. Aratani, A. Osuka, *J. Phys. Chem. B* **2005**, *109*, 8643.

[22] S. E. Bradforth, R. Jimenez, F. van Mourik, R. van Grondelle, G. R. Fleming, *J. Phys. Chem.* **1995**, *99*, 16179.

Received: November 4, 2005
Published online: January 9, 2006

